Monitoring the Effects of Selective Laser Sintering (SLS) Build Parameters on Polyamide Using Near Infrared Spectroscopy

M. A. Beard, O. R. Ghita, K. E. Evans

College of Engineering, Mathematics and Physical Sciences, University of Exeter, United Kingdom

Received 29 July 2010; accepted 25 November 2010
DOI 10.1002/app.33898
Published online 6 April 2011 in Wiley Online Library (wileyonlinelibrary.com).

ABSTRACT: Near infrared spectroscopy has been used to monitor the effects of changing build parameters on the sintering process of selective laser sintering components. The surface roughness of the parts produced has been studied whilst modifying laser scan speed and laser power build parameters. Near infrared spectroscopy is shown to be a powerful tool in detecting subtle variations in the coalescence of particles that form the surface topology of the component. Principal component analysis (PCA) performed on the diffuse reflectance spectra obtained from the surface of the components shows a strong correlation between near infrared (NIR) spectra and build parameters. Using the chemometric model produced from the PCA analysis it is possible to calculate build parameters for unknown components, making NIR a useful aid for quality control of additive manufacturing technologies. © 2011 Wiley Periodicals, Inc. J Appl Polym Sci 121: 3153–3158, 2011

Key words: selective laser sintering; near infrared spectroscopy; polyamide; SLS; build parameters

INTRODUCTION

Additive manufacturing is an emerging technology that is becoming increasingly adopted in a broad sector of manufacturing industries that range from aerospace to healthcare.[1] Amongst additive manufacturing techniques, selective laser sintering (SLS)[2] is one of the most established and readily available. Therefore, SLS has attracted the most academic study of additive manufacturing technologies with research being conducted into part analysis and process optimization, and also hardware and software development.[2–4]

Normally, the SLS process uses a focused laser to selectively sinter parts. The laser spot rasters a pattern of a single layer of the component on a polymeric powder bed. The bed lowers slightly and a new layer of powder is applied. This additive process is then repeated until all layers are complete and the final component constructed. The SLS process is complex; the properties of parts obtained are directly dependent on initial material properties, such as particle size and shape, and also machine parameters such as part bed temperature, laser scanning speed, laser power, layer thickness, and laser spot size. Any change in machine or material parameters will ultimately affect the sintering process, material molecular structure, and subsequently the mechanical properties of the obtained parts. Such effects had been previously investigated by Kruth et al.,[5] when analyzing the effect of laser power on polyester based elastomers. Their study showed an increase in the hardness and elongation of the obtained parts with increase of laser power. Similarly, Ho et al.,[6] reported on the effects of energy density on morphology and properties of polycarbonate processed by SLS. High laser energy density resulted in improved fusion and compact polycarbonate structures, although excessively high energy density caused degradation of the polymer. Caulfield et al.[3] carried out an extensive study on the effect of energy density on the physical and mechanical properties of polyamide components. The tensile testing results revealed an increase in Young's modulus and elongation at break with increasing energy density level.

To develop parts of highest mechanical performance with good dimensional accuracy and repeatability, all studies to date have focused directly on mechanical analysis without an in-depth analysis of the molecular changes suffered by polymeric material during the sintering process. Thermal analysis (DSC) has been employed in various studies and has provided useful information on the crystallinity or degradation of sintered parts,[5,7] but the data refers only to the bulk properties of the sample.

When it comes to identifying and monitoring structural changes of polymers due to chemical or

Correspondence to: M. A. Beard (m.a.beard@ex.ac.uk).

physical changes, spectroscopy is one of the most powerful techniques available as it can provide direct information on specific vibrational bonds within a molecule. Raman spectroscopy has been successfully used in the past for analysis of bulk nylon structures.[8,9] Hendra et al.,[8] showed that Raman spectroscopy can differentiate even between different types of nylon (nylon 3 to nylon 12 and polyethylene) by analyzing peaks intensities associated with stretching and bending vibrational modes of CH_2 chains.

This study demonstrates that variations in laser scan speed and laser power within the SLS manufacturing process can be identified by near infrared (NIR) spectroscopy analysis of the manufactured component. Principle component analysis (PCA) highlights the strong correlation between the laser scan speed and laser power used in the SLS process and the predicted values obtained from the measured near infrared spectra. It is shown that the changes in the NIR diffuse reflectance spectra are due to changes in surface scatter from the SLS components which in turn is related to the degree of particle coalescence during the sintering process.

SELECTIVE LASER SINTERING - PARTS MANUFACTURING

All parts were manufactured on a DTM Sinterstation using DuraForm polyamide powder provided by 3D Systems.[10] To avoid any effects due to temperature variation across the powder bed, all samples were built in the center of the build area one on top of each other. Tests specimens of 20 mm × 20 mm × 2 mm were manufactured with a laser fill scan spacing of 0.15 mm. For the first set of samples, the laser fill speed was varied from 800 to 1600 mm/s, with the laser power being kept constant at 5 W. The second set of samples was manufactured using a constant laser scan speed of 1200 mm/s and the laser power varied between 3 and 7 W.

EXPERIMENTAL METHODS

Infrared spectroscopy

All spectra were measured using a Bruker Matrix spectrometer and a reflectance bifurcated optical fiber probe operating in the near infrared region from 4000 to 10,000 cm^{-1}. Spectra were collected at 4 cm^{-1} resolution using a white light source, a CaF2 beamsplitter and a TE-InGaAs detector. Principal component analysis was performed on the spectra using OPUS software by Bruker Optics UK.[11] Due to surface finish obtained from components manufactured using the SLS process, spectra were considered to be diffuse reflectance measurements where the light is diffusely scattered by the sample. Therefore,

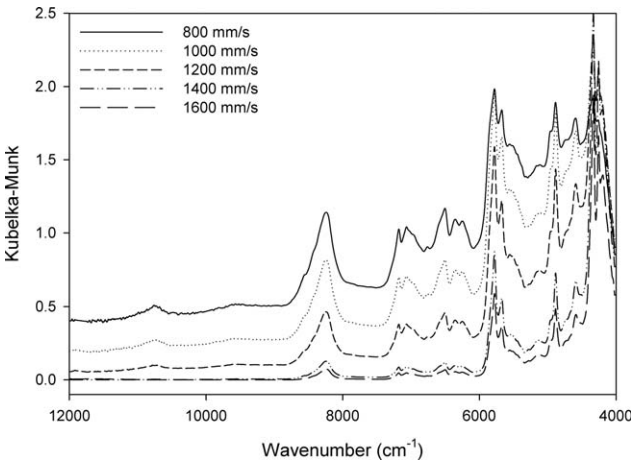

Figure 1 Near infrared KM spectra of polyamide samples manufactured at varied laser scan speeds.

to correctly account for the optical properties of the scattered light, all reflectance near infrared spectra were converted within the OPUS software to Kubelka-Munk (KM) units using the KM equation[12]:

$$F(R) = \frac{(1 - R^2)}{2R} = \frac{K}{S} \quad (1)$$

where R is the diffuse reflectance, K is the absorption coefficient and S is the scattering coefficient which depends on the number, size, shape and reflectivity of the particles.

Scanning electron microscopy

The SEM examination of the SLS manufactured samples was performed using a Hitachi S-3200N scanning electron microscope (SEM). All samples were coated with a 4 nm gold coating to reduce surface charging and secondary electron images were taken with an accelerating voltage of 25 kV.

RESULTS AND DISCUSSION

Figure 1 shows the near infrared spectra of polyamide samples manufactured at 800, 1000, 1200, 1400, and 1600 mm/s scan speeds and a constant laser fill power of 5 W. It can be observed that the near infrared spectra show an overall baseline shift which makes it difficult to distinguish and identify any other changes between samples. For this reason, the first derivative of these spectra was calculated to enhance spectral features produced by the modifications made by varying laser can speed and is shown in Figure 2.

In Figures 1 and 2, the 6000–5500 cm^{-1} region is associated with the stretching vibrations of the C—H within the —CH_2, —CH bands of polyamide.[13] The

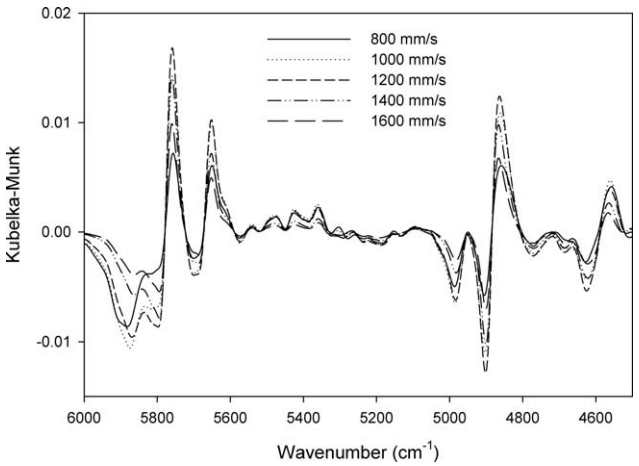

Figure 2 First derivate spectra of polyamide samples manufactured at varied laser scan speeds.

region 5050–4500 cm^{-1} represents the combination bands of C=O and the NH— stretching vibrations combined with the —CH_2 and —CH bending vibrations. The first derivative conversion in the 6000–5500 cm^{-1} stretching vibration region revealed the presence of a larger number of additional peaks than the doublet shown by the KM spectra. This is not surprising as several previous near infrared studies of nylon[13,14] reported also the presence of four[13] or at least five[14] peaks in the stretching vibration region. Clear changes in the 5775 cm^{-1} peak intensity as a function of laser scan speed can also be noticed in Figure 2. The sample sintering temperature is possibly slightly increased at low scan speeds which induces increased molecular mobility resulting in further crystallization or recrystallization that is reflected by changes in this associated peak. Previous premelting investigations of nylon 12 using two dimensional (2D) NIR[15] had similar conclusions. However, cross-linking mechanisms can not be excluded as a possibility either.[16,17]

The KM spectra shown in Figure 1 clearly show the dependence that the absorbance has on the laser scan speed. The absorbance is shown to decrease with an increasing scan speed. To help explain this effect, it is important to understand the sintering process. The starting material is a polyamide powder with an average particle size of 58 μm.[10] The build parameters are set and the laser in the SLS process selectively scans the powder bed. The laser provides the extra heating required to allow the particles to sinter. A slow scan speed will allow particles to fully fuse and will lead to a smoother surface finish. Where as a fast scan speed will limit coalescence of the particles and the component surface will resemble the initial surface of the powder. In this case, the scattering coefficient S in eq. (1) is the predominant term which affects the K/S ratio and ultimately a lowering of the KM absorbance. Lower scan speeds produces a smoother surface with lower scattering effects causing a higher K/S ratio which corresponds to an increase in peak intensity. To help illustrate this relationship, SEM images were taken of components manufactured at three specific laser fill speeds: 800, 1200, and 1600 mm/s and are shown in Figure 3.

The SEM images shown in Figure 3 confirm that at high scan speeds the surface of the manufactured part is rougher with minimal coalescence between particles. The initial particle size and shape of the powder can still be clearly distinguished. At slow scan speeds the surface is considerably smoother with strong interparticle neck growth. The SEM images help to understand the relationship between the observed peak intensity effects of the NIR spectra and the surface scatter of the SLS components.

Based on the infrared intensity effects and the SEM results, multivariate analysis was used to determine whether the scattering effects could be used as a monitoring criterion in SLS process. Standard univariate methods for quantitative analysis cannot be applied in this case as there are no isolated spectral bands related specifically with the scattering effects. Therefore, principal component analysis was performed using the Bruker OPUS software. PCA can

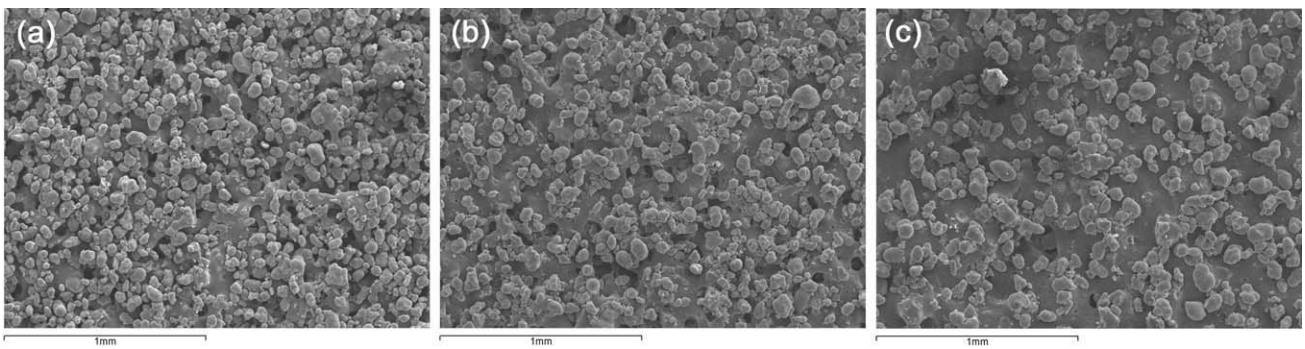

Figure 3 SEM images of SLS manufactured parts manufactured at (a) 1600 mm/s, (b) 1200 mm/s and (c) 800 mm/s scan speed and constant laser fill power of 5 W

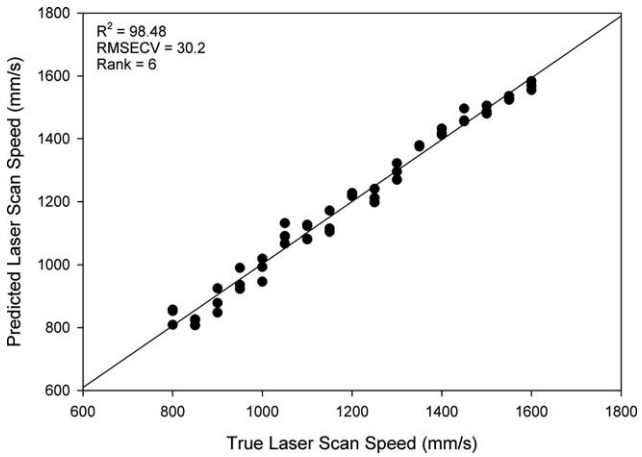

Figure 4 Cross-validation graph showing predicted against true laser scan speed.

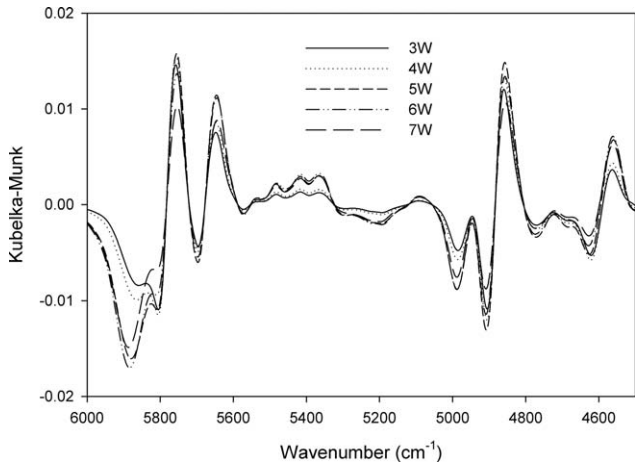

Figure 6 First derivative near infrared KM spectra of polyamide samples manufactured at varied laser powers.

be performed over a large spectral range providing a more robust and accurate model than standard univariate methods. The quality of the PCA analysis can be further improved with large data sets. For this reason, three NIR spectra were acquired for each of 17 different sample manufactured at scan speeds ranging from 800 to 1600 mm/s at 50 mm/s intervals, producing a total of 51 spectra. Multiplicative scattering correction has been used as preprocessing method, which performs a linear transformation of each spectrum for it to best match the average spectrum of the whole set. This method is often used for spectra measured in diffuse reflection. The accuracy of the chemometric model produced by PCA can be evaluated by a cross validation graph showing true scan speed versus near infrared predicted scan speeds and is shown in Figure 4.

In Figure 4, the determination coefficient, R^2, gives the percentage of variance present in the true component values; R^2 approaches 100% as the fitted values approach the true values. The RMSECV corresponds to root mean square error of the cross-validation model, and the rank is related to the number of PCA vectors used. A good correlation between the true scan speed values and the ones predicted by the near infrared spectra has been obtained all across the scan speed range, with slightly more variation in the data at lower scan speeds.

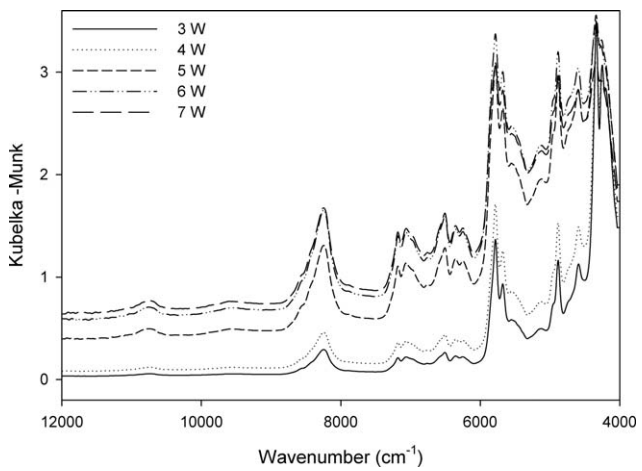

Figure 5 Near infrared KM spectra of polyamide samples manufactured at varied laser powers.

In addition to the laser scan speed, the effect of the laser power variation on the near infrared spectra has been investigated. Figures 5 and 6 show the KM spectra and the first derivative for five components manufactured at varied laser powers. A trend of increasing intensity with increasing laser power can be observed from the spectra. However, the highest power spectra recorded at 6 and 7 W show almost no difference in intensity. It is possible that for the high power range the actual laser power reaches a physical upper limit or more likely it is due to a sintering rate reduction due to the complex neck growth kinetics.[5] It can also be seen that the first derivative spectra has revealed subtle molecular changes in the 6000–5500cm^{-1} region, similar to that observed with the scan speed.

SEM images of the 3, 5, and 7 W laser power samples are shown in Figure 7. The effect the laser power has on the sintering process can clearly be observed though changes in the surface topology of the samples. In a result similar to that observed with the laser scan, increases in laser power have produced better particle consolidation and smoother surface finish.

Principal component analysis was performed on 17 components where the laser power ranged from 3 to 7 W in increments of 0.25 W. Three spectra for each component were measured and the results of the cross validation graph are shown in Figure 8.

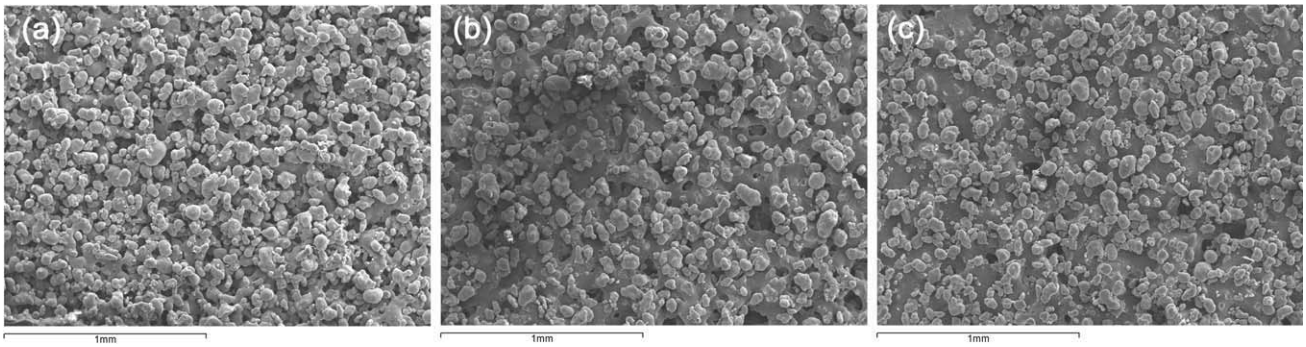

Figure 7 SEM images of SLS manufactured parts manufactured at (a) 3 W, (b) 5 W and (c) 7 W laser fill power and constant scan fill speed of 1200 mm/s

The cross-validation between the true laser power and the values predicted by the near infrared shows a larger variation than the one obtained for the scan speed. This is reflected by the lower R^2 value of 94.6 for the laser power cross-validation as compared to 98.5 for laser scan speed cross-validation. Although a strong correlation can still be seen, the cause of the lower R^2 value is increased scatter between spectra recorded from the same component. This is believed to be the accuracy, and inherent difficulty, of controlling the SLS laser in increments of 0.25 W between successive runs.

To directly compare the machine parameters effects of laser scan speed and laser power it is useful to convert these parameters into laser energy density[2,17] using eq. (2):

$$\text{Laser energy density} = \frac{P}{vd} \tag{2}$$

where, P is the laser power, v is the scan speed and d is the laser fill scan spacing. The laser energy density is the overall energy input applied to the powder bed during sintering. Higher energy density leads to lower porosity, higher mechanical properties and high shrinkage effects when energy is too high.[17] The relationship between the laser scan speed and laser power compared to the laser energy density is shown in Figure 9.

Having converted the two sets of parameters it was then possible using PCA to combine all spectra into a single chemometric model. The resulting single cross-validation curve is shown in Figure 10.

The combined chemometric model gives comparable results with the individual cross-validations graphs for laser power and scan speed show in Figures 4 and 8. A strong correlation can still observed in the PCA analysis between the two set of manufactured components. This highlights that the laser energy density would serves as a better single representative measure of the degree of consolidation between different SLS machines than individual machine parameters alone. The high R^2 value of the laser scan speed cross-validation would indicate that modification and control of this build parameter is more stable than controlling laser power. So for the SLS machine used to manufacture the components

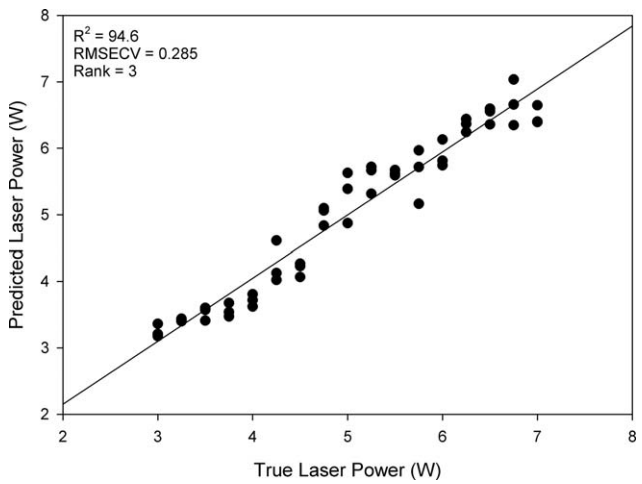

Figure 8 Cross-validation graph showing predicted against true laser power.

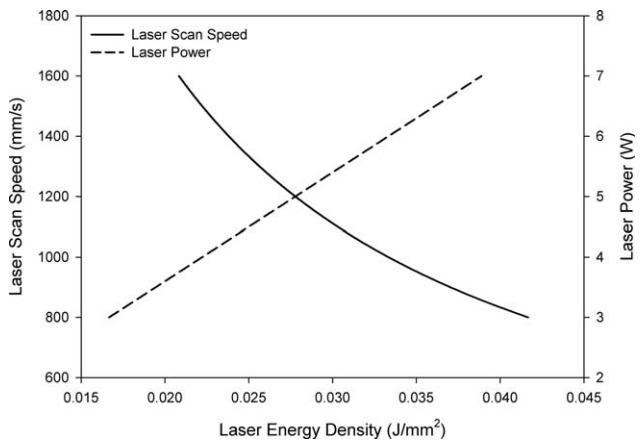

Figure 9 Graph showing the laser power and laser scan speed as a function of laser energy density

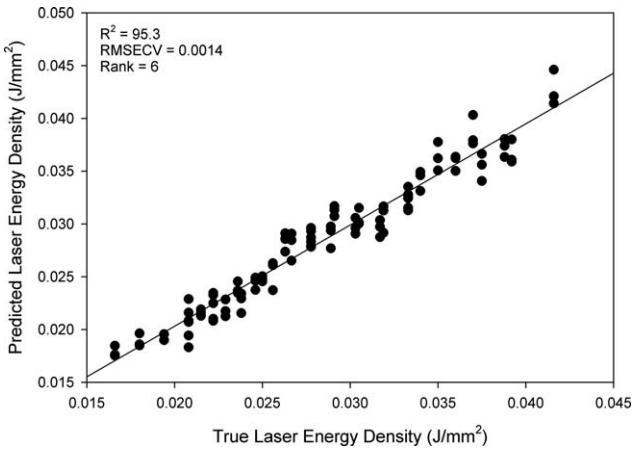

Figure 10 Cross-validation graph showing predicted against true laser energy density.

described in this article, it is more repeatable to alter the laser scan speed than the laser power, to achieve a desired coalescence of particles.

CONCLUSIONS

The results presented in this study demonstrate the potential offered by near infrared spectroscopy to monitoring build parameters in additive manufacturing processes. The chemometric models produced by PCA have shown a strong correlation between the changes in NIR spectra and changes in laser energy density during the build process. This is attributed to changes in the diffuse scatter from the surface of the samples. Samples with build parameters that cause increased coalescence between particles have a smoother surface finish causing lower diffuse reflectance of light, while the surface of samples manufactured at lower laser energy density levels are rougher and show increased diffuse reflectance levels. It was noticed that between the two build parameters studied, the laser scan speed gave more control and repeatability of the sintering process.

NIR spectroscopy has the potential to provide better understanding and optimization of the entire SLS process. This study has demonstrated that it is an accurate and feasible method to determine the quality of AM parts. NIR has the potential for off-line or in-line component analysis and could even be used to identify build parameters of unknown SLS components.

References

1. Wohlers, T. In Wohlers Report 2009; Wohlers: Colorado, 2009.
2. Beal, V. E.; Paggi, R. A.; Salmoria, G. V.; Lago, A. J Appl Polym Sci 2009, 113, 2910.
3. Caulfield, B.; McHugh, P. E.; Lohfeld, S. J Mater Process Technol 2007, 182, 477.
4. Tang, Y.; Loh, H. T.; Fuh, J. Y. H.; Wong, Y. S.; Lu, L.; Ning, Y.; Wang, X. 2003. http://hdl.handle.net/1721.1/3898.
5. Kruth, J. P.; Levy, G.; Klocke, F.; Childs, T. H. C. CIRP Ann Manuf Technol 2007, 56, 730.
6. Ho, H. C. H.; Gibson, I.; Cheung, W. L. J Mater Process Technol 1999, 89, 204.
7. Albano, C.; Sciamanna, R.; Gónzalez, R.; Papa, J.; Navarro, O. Eur Polym J 2001, 37, 851.
8. Hendra, P. J.; Maddams, W. F.; Royaud, I. A. M.; Willis, H. A.; Zichy, V. Spectrochimica Acta Part A 1990, 46, 747.
9. Nagae, S.; Nakamae, K. Int J Adhes Adhesives 2002, 22, 139.
10. 3D Systems. Duraform PA Data Sheet. http://www.3dsystems.com/products/datafiles/lasersintering/datasheets/DS-DuraForm_PA_plastic-A4_UK.pdf, 2006.
11. Bruker Optics UK. www.brukeroptics.com/uk/.
12. Szalay, A.; Antal, I.; Zsigmond, Z.; Marton, S.; Er, I.; odblac, G. R., Jr.; Pintye-Hódi, K. Part Part Syst Char 2005, 22, 219.
13. Wu, P.; Yang, Y.; Siesler, H. W. Polymer 2001, 42, 10181.
14. Ozaki, Y.; Liu, Y. L.; Noda, I. Macromolecules 1997, 30, 2391.
15. Peebles, L. H.; Huffman, M. W. J Polym Sci Part A-1: Polym Chem 1971, 9, 1807.
16. Levchik, S. V.; Levchik, G. F.; Balabanovich, A. I.; Camino, G.; Costa, L. S Polym Degrad Stabil 1996, 54, 217.
17. Yusoff, W. A. Y.; Thomas, A. J. In Proceedings of the IAMOT 2008 International Association for Management of Technology, Dubai; 2008.